Antiatherogenic effects of ellagic acid and urolithins in vitro

ANTIATHEROGENIC EFFECTS OF ELLAGIC ACID AND UROLITHINS *IN VITRO*

Laura Mele[1], Pedro Mena[1], Antonio Piemontese[2], Valentina Marino[2], Noelia López-Gutiérrez[3], Franco Bernini[2], Furio Brighenti[1], Ilaria Zanotti[2*], Daniele Del Rio[1,4*]

[1] Human Nutrition Unit, Department of Food Science, University of Parma, Via Volturno 39, 43125 Parma, Italy.

[2] Department of Pharmacy, University of Parma, Viale delle Scienze 27a, 43124 Parma, Italy.

[3] Group "Analytical Chemistry of Contaminants", Department of Chemistry and Physics (Analytical Chemistry Area), University of Almería, Carretera de Sacramento s/n, E-04120 Almería, Spain.

[4] The Need for Nutrition Education/Innovation Programme (NNEdPro), University of Cambridge, Cambridge, UK.

* Corresponding authors. Address: Department of Pharmacy, University of Parma Viale delle Scienze 27a, 43124 Parma, Italy. Fax: +39 0521 905040 (I. Zanotti). Address: The Laboratory of Phytochemicals in Physiology, Human Nutrition Unit, Department of Food Science, Medical School Building C, Via Volturno 39, University of Parma, 43125 Parma, Italy. Fax: +39 0521 903832 (D. Del Rio). E-mail addresses: ilaria.zanotti@unipr.it (I.Zanotti), daniele.delrio@unipr.it (D. Del Rio).

Abstract

Atherosclerosis, one of the leading causes of death worldwide, is characterized by impaired endothelial function and lipid metabolism, among other factors. Ellagitannins are a class of phenolic compound that may play a role in cardiovascular health. This work aimed to study the potential atheroprotective effects of urolithins, ellagitannin-derived gut microbiota metabolites, on different key factors in atherosclerosis development: the ability of monocytes to adhere to endothelial cells and the uptake and efflux of cholesterol by macrophages. The biotransformations urolithins may undergo in peripheral cells were also evaluated. Results indicated that some urolithins and ellagic acid, at physiologically relevant concentrations, were able to reduce the adhesion of THP-1 monocytes to human umbilical vein endothelial cells (HUVECs) and the secretion of a cellular adhesion molecule (sVCAM-1) and pro-inflammatory cytokine (IL-6). Urolithin C, a combination of urolithins A and B, and ellagic acid also decreased the accumulation of cholesterol in THP-1-derived macrophages treated with hypercholesterolemic serum and acetylated LDL, but they were not able to promote cholesterol efflux. The analysis of cell media by UHPLC-ESI-MS^n indicated urolithins and ellagic underwent extensive metabolism within vascular cells, representing significant sulfate and methyl conjugation. This evidence indicates atherosclerotic processes may be attenuated by urolithins following ellagitannin consumption, however, future human intervention trials are required to establish if regular intake of ellagitannin-rich foodstuffs attenuates atherosclerotic.

Keywords: atherosclerosis, cholesterol transport, endothelial function, ellagitannin metabolites, urolithins, peripheral metabolism

1. Introduction

Atherosclerosis is a chronic disorder caused by multiple factors that impair vascular function and damage the artery wall. Dysfunctional endothelium, characterized by increased expression of cell adhesion molecules such as vascular cell adhesion molecule-1 (VCAM-1) and intercellular adhesion molecule-1 (ICAM-1), allows accumulation of monocytes in the subendothelial matrix. Infiltrated monocytes differentiate into cells with macrophage and/or dendritic cell-like features. Uptake of oxidized low density lipoprotein (oxLDL) and native LDL by these cell types (via scavenger receptors or fluid phase pinocytosis, respectively), leads to foam cell formation [1, 2]. The presence of lipid-rich foam cells contributes to plaque formation and eventually progresses to the clinical presentation of atherosclerosis [3].

Ellagitannins are a subclass of hydrolysable tannins characterized by the presence of ellagic acid (EA) and glucose [4]. They are mostly found in fruits such as pomegranate, raspberries, strawberries, blackberries, blueberries, muscadine grapes and persimmon, nuts including walnuts, pistachio, cashew, and hazelnuts, and oak-aged wines (where tannins are released from the barrels) [5]. For the past decade, many studies have focused on the *in vitro* atheroprotective effect of ellagitannin-rich extracts. Ellagitannin extracts have been reported to delay LDL oxidation [6] and to reduce cholesterol accumulation in macrophages, both inhibiting the uptake and stimulating high density lipoprotein (HDL) efflux [7]. Ellagitannins have been shown to improve vascular function through inducing the expression of endothelial nitric oxide synthase (eNOS) in human artery endothelial cells [8, 9], inhibiting platelet aggregation and monocyte adhesion to endothelial cells, and reducing the expression of ICAM-1 and VCAM-1 in human endothelial cells [10]. Some of these protective effects were confirmed *in vivo* in animal and human studies, where consumption of ellagitannins from different sources was mostly associated with improvement of serum lipid profile and antioxidant activity [11, 12]. However, the number of intervention studies conducted to date is limited and most of the *in vitro*

studies have been poorly designed, since cells of the vascular system were exposed to plant extracts rich in ellagitannins, which are unlikely to reach the systemic circulation after consumption of ellagitannin-containing foodstuffs [5, 11]. It now established that ellagitannins are hydrolyzed in the small intestine, releasing EA; the free EA is poorly absorbed and more than 99% of it is metabolized by the gut microbiota, forming the bioavailable urolithins. Urolithins are molecules characterized by a common 6*H*-dibenzo[*b*,*d*]pyran-6-one nucleus and a decreasing number of phenolic hydroxyl groups (urolithin D → C → A → B) [13, 14]. They can be further metabolized by phase II enzymes (methylation, glucuronidation and sulfation), mainly by enterocytes and hepatocytes, and appear in circulation at low micromolar concentrations [15].

Despite a limited number of studies attempting to elucidate the anti-inflammatory properties of urolithins in endothelial cells and macrophages [16, 17], very little is known about the preventive role of urolithins in atherosclerosis. Therefore, the aim of the present study was to evaluate the potential atheroprotective effects of urolithins with diverse patterns of hydroxylation, on different key atherogenic processes, namely monocyte adhesion to endothelial cells and cholesterol transport. Distinct emphasis was placed on the ability of urolithins to promote cholesterol efflux, a strong predictor of the extent of atherosclerosis, which is inversely associated to cardiovascular risk [18, 19]. This work also aimed to identify the cellular mechanisms underlying the cardioprotective effects of ellagitannin-containing foodstuffs. Moreover, considering the extensive biotransformations that urolithins are likely to undergo in peripheral cells [20], the metabolism of these ellagitannin-derived molecules in the applied cell models was studied.

2. Material and methods

2.1. Materials

Fetal calf serum (FCS), bovine serum albumin (BSA), Acyl CoA:cholesterol acyltranferase (ACAT) inhibitor, DNase, phorbol, 12-myristate, 13-acetate (PMA), and bovine skin-derived gelatin solution were purchased from Sigma-Aldrich (St. Louis, MO, USA). RPMI/HEPES culture medium and PBS were from Lonza (Walkersville, MD, USA). Tumor Necrosis Factor-α (TNF-α), Medium 200, Low Serum Growth Supplement Kit, Amplex Red Cholesterol Assay Kit, soluble VCAM-1 (sVCAM-1) ELISA kit, and IL-6 ELISA kit from Thermo Fisher Scientific (Waltham, MA USA). [1,2-^{3}H]cholesterol was obtained from PerkinElmer (Boston, USA). Human LDL were kindly provided by Prof. Calabresi (University of Milan, Italy) and were acetylated (acLDL) according to Basu et al. [21]. Human serum was collected with approved consent from healthy normolipidemic individuals. Hypercholesterolemic serum was collected with informed consent from patients affected by familial hypercholesterolemia at the Reference Center for Hereditary Dyslipidaemias (Pisa, Italy) and pooled.
Urolithin A (Uro A) and urolithin B (Uro B) were provided by Prof. O. Dangles (INRA, Avignon, France), while urolithins C and D (Uro C and Uro D) were purchased from Dalton Pharma Services (Toronto, ON, Canada). EA was from Sigma-Aldrich. All solvents and reagents for extraction and UHPLC-MS analysis were purchased from Carlo Erba Reagents (Milan, Italy).

2.2. **Cells**

Human Umbilical Vein Endothelial Cells (HUVECs) were purchased from GIBCO, Life Technologies (Frederick, MD, USA) and cultured in Medium 200 supplemented with Low Serum Growth Supplement Kit (as recommended by the manufactory). HUVECs were used for experiments between II and V passage.
Human monocytes-derived macrophages THP-1 were purchased from ATCC (Teddington, UK) and cultured in RPMI/HEPES supplemented with 1 mM sodium pyruvate, 50 μM β-mercaptoethanol, 2.5

mg/mL glucose and 10% FCS. Differentiation into macrophages was obtained by treating cells with 50 ng/mL of PMA for 72 h.

2.3. Monocyte adhesion to endothelial cells

HUVECs were grown on gelatin-coated 96-well plates (30.000 cells/well) until confluence. Cells were treated with or without urolithins A, B, C, and D, and EA at 10 µM for 6 h. An association of Uro A and Uro B at 10 µM each (named Uro A+Uro B, 10 µM) was also tested. During the last 2 h of treatment, cells were incubated with 15 ng/mL TNF-α. THP-1 monocytes were labeled with 5 µM calcein and a cell suspension was added to the HUVECs monolayers (50.000 cells/well). Cells were co-incubated for 30 min, following rinsing of unbound THP-1 and subsequent determination of adherent cells fluorometrically. Results were expressed as percentage of adherence of control TNF-α treated cells.

2.4. IL-6 and sVCAM secretion in endothelial cells

HUVECs were seeded on gelatin-coated 24-well plates (180.000 cells/well) until confluence. Cells were pre-treated with or without Uro C, Uro D, association of Uro A and Uro B (Uro A+Uro B), and EA at 10µM for 6 h. After 18 h incubation with the treatments and 15 ng/mL TNF-α, cell supernatants were collected and immediately frozen at -80 ºC. IL-6 and sVCAM protein levels were quantified in HUVEC cell surnatants by using commercial enzyme-linked immunosorbent assays, according to the manufacturer's instructions. Results of IL-6 and sVCAM were expressed as pg/mL and ng/mL, respectively.

2.5. Macrophage cholesterol loading

THP-1-derived macrophages were cultured in the presence of human hypercholesterolemic serum (HCS) (5%, v/v) or acetylated LDL (acLDL) (50 µg/mL) to induce foam cell formation, with or without urolithins A, B, C, and D, combination of Uro A and Uro B (Uro A+Uro B), and EA at 10 µM. After 24 h cells were lysed using 1% sodium cholate and DNAse (50 U/mL). Cholesterol was measured by fluorimetric analysis with the Amplex Red Cholesterol Assay Kit, according to manufactures instructions. The amount of cholesterol in each well was corrected for the protein content of the well and successively expressed as percentage of cholesterol content of control cholesterol-loaded cells. Protein content in the lysate was measured by the use of bicinchoninic acid assay [22]. The same protocol was used to evaluate the effect of the treatments on cholesterol content in THP-1-derived macrophages before exposure to HCS or acLDL.

2.6. Macrophage cholesterol efflux

Cholesterol efflux from THP-1-derived macrophages was evaluated using a radioisotope assay [23]. Briefly, cells were radiolabeled with 2 µCi/mL [1,2-^{3}H]cholesterol in presence of ACAT inhibitor (2 µg/mL) for 24 h. Successively, cells were incubated for 18 h in culture medium supplemented with 0,2% (w/v) of BSA and ACAT inhibitor (2µg/ml) in presence or absence of human HCS (5%, v/v) or acLDL (50 µg/mL), and Uro C, Uro D, combination of Uro A and Uro B (Uro A+Uro B), and EA at 10 µM. Cholesterol efflux was promoted to human normocholesterolemic serum (NCS) (2%, v/v) for 4 h. Efflux was expressed as a percentage of ^{3}H-cholesterol released in the medium relative to the total amount incorporated by cells.

2.7. Ultra-high performance liquid chromatography coupled to mass spectrometry (UHPLC-MS^{n}) analysis of cell media

158 Cell culture supernatants were collected at the end of the experiments and analyzed by UHPLC-MS^n to
159 determine the stability and peripheral metabolism of the urolithins in cell media. Cell media was
160 extracted according to Sala et al. [20] and analyzed according to Sala et al. [20]; with minor
161 modifications. Briefly, samples were analysed using an Accela UHPLC 1250 equipped with a linear
162 ion trap-mass spectrometer (LTQ XL, Thermo Fisher Scientific Inc., San Jose, CA, USA) fitted with a
163 heated-electrospray ionization probe (H-ESI-II; Thermo Fisher Scientific Inc.). Separations were
164 performed using a XSELECTED HSS T3 (50x2.1 mm), 2.5 µm particle size (Waters, Milford, MA,
165 USA), with an injection volume of 5 µL, column oven temperature of 30°C and elution flow rate of 0.2
166 mL/min. The initial gradient was 75% of 0.1% aqueous formic acid and 25% acetonitrile (in 0.1%
167 formic acid), reaching 80% acetonitrile at 6 min. The MS conditions included: capillary temperature of
168 275 °C and source heater temperature of 250 °C, sheath gas flow of 40 units, auxiliary and sweep gas
169 of 5 units, source voltage of 3 kV and capillary voltage and tube lens of -5 and -68 V, respectively.
170 Analyses were carried out using full scan, data-dependent MS^3 scanning from *m/z* 100 to 600, with
171 collision induced dissociation (CID) equal to 35 (arbitrary units). Pure helium gas was used for CID.
172 Data processing was performed using Xcalibur software from Thermo Scientific.
173
174 **2.8. Statistical analyses**
175 Statistical analysis was assessed using Prism 5.0 (GraphPad Inc., San Diego, CA, USA). Comparisons
176 among means were performed with one-way ANOVA followed by Newman-Keuls Multiple
177 Comparison Test. Significant differences were defined as $p < 0.05$.
178
179 **3. Results**
180 **3.1. Effect of ellagitannin metabolites on human endothelial cells**

To determine whether urolithins or EA could exert anti-inflammatory effects on the human endothelium, their impact on the capacity of monocytes to adhere to endothelial cells was tested. HUVECs were treated with non-cytotoxic concentrations of ellagitannin metabolites (10 µM), as demonstrated by protein content of cellular lysates, which did not show significant differences among treatments (Table 1). The effect of ellagitannin metabolites on the adhesion of THP-1 monocytes to HUVEC is showed in Fig. 1. Exposure of HUVEC monolayers to 15 ng/mL of TNF-α for 2 h caused a 4-fold increase in monocyte adhesiveness compared to untreated cells ($p < 0.001$). Treatment with single urolithins at 10 µM for 6 h slightly reduced the adhesion of THP-1 monocytes to HUVECs (Uro D, -23.2%; Uro C, -24.7%; Uro A, -26.7%; Uro B, -10.7%; not significant). The effect co-treatment with 10 µM of both Uro A and Uro B significantly limited monocyte adhesiveness compared with cells treated only with TNF-α (-39.8%, $p < 0.05$). However, this anti-adhesive effect was lost at the dose of 5 µM each one. A similar effect was observed for EA: the treatment with 10 µM significantly reduced monocyte adhesion to HUVECs (-29.3%, $p < 0.05$), while at 5 µM there was no effect.

Since the interaction between endothelium and monocytes is dependent on the expression of adhesion molecules on cell surface [1], the effect of urolithins and EA on VCAM-1 expression in HUVEC was investigated. Assay optimization involved a preliminary experiment establishing the time-course of TNF-α-induced sVCAM-1 secretion (data not shown); where 18h stimulation with TNF-α was established as optimal (i.e., maximum sVCAM-1 protein response). Subsequently, EA, Uro D, and Uro C were tested as distinct molecules at 10 µM, whereas Uro A and Uro B were in mixture, but not individually, as the combination influenced monocyte adhesion in previous experiments (Fig. 1). In these experimental conditions (Fig. 2A), incubation with TNF-α caused a significant increase in sVCAM-1 secretion (250-fold higher than non-treated, $p < 0.001$) that was partially reduced by EA (-25,6%, $p < 0.05$) and, to a lesser extent, by Uro C (-17,5%, $p = 0.08$).

To evaluate whether the anti-adhesive effect of some ellagitannin metabolites was associated with a reduction in the secretion of inflammatory cytokines, IL-6 was quantified (Fig. 2B). Interestingly, both Uro C and EA significantly reduced the secretion of IL-6 (-36.2% and -39.7%, respectively; $p < 0.05$). in comparison to the cells treated with TNF-α alone.

3.2. Effect of ellagitannin metabolites on macrophage cholesterol accumulation

The role of urolithins in the uptake and efflux of cholesterol from macrophages was investigated as a key factor in plaque development [18]. Uptake experiments (Fig. 3) involved THP-1 macrophages treated with non-cytotoxic concentrations of ellagitannin metabolites, as demonstrated by the protein content of cellular lysates treated at 10 µM. No significant differences among the treatments were observed (Table 2). Incubation of cells with hypercolesterolemic serum (HCS) for 24 h increased cholesterol content 1.5 fold (p <0.001, Fig. 3A). Co-incubation of HCS and Uro C at 10 µM and 5 µM reduced cholesterol accumulation to a similar extent (21.3% and 18.6%, respectively; $p < 0.01$), whereas the lowest dose (1 µM) was ineffective. The EA dosage reduced cholesterol accumulation in a concentration dependent manner: -16.9% ($p < 0.01$), -9.7% ($p < 0.05$), and -4.2% ($p = 0.45$) at 10, 5, and 1 µM, respectively (Fig. 3A). Conversely, the other urolithin treatments had no impact on cholesterol loading induced by HCS. Alternatively, incubation of THP-1 macrophages with acetylated LDL (acLDL) increased cell cholesterol content 1.9-fold, with respect to untreated cells ($p < 0.001$), however, neither Uro C nor EA at 10 µM were able to attenuate cholesterol accumulation (Fig. 3B). Nevertheless, the simultaneous treatment with Uro A and Uro B significantly limited cholesterol accumulation at the highest concentration, 10 µM (-29.3%, $p < 0.001$; Fig. 3B).

As cellular cholesterol content is the net result of a bidirectional flux of cholesterol mediated by lipoproteins [24], the observed effect on cellular cholesterol content could be related either to a reduction in cholesterol uptake or to a promotion of cholesterol efflux. Therefore, the effect of

metabolites on reducing cellular cholesterol content by improving cholesterol efflux was assessed (Fig. 4). THP-1 macrophages were treated for 18 h with cholesterol donors (HCS or acLDL) in order to induce foam cell formation in either the presence or absence of urolithins or EA. Subsequent incubation with normocholesterolemic serum (NCS)-containing medium promoted cholesterol efflux (3.3-fold increase) in HCS pre-treated cells ($p < 0.001$, Fig. 4A) and 6-fold increase in acLDL pre-treated cells ($p < 0.001$, Fig. 4B), compared to cells incubated with serum-free medium during the efflux period (Basal treatment). However, none of the treatments with urolithins significantly affected cholesterol efflux (Fig. 4).

As all mammalian cells synthesize cholesterol [25], in addition to uptake and efflux experiments, the effect of the tested metabolites was also evaluated on basal cellular cholesterol levels (i.e., content before the addition of cholesterol). There was no effect of urolithins or EA at 10 μM on cellular cholesterol content (Table 3).

3.3. *In vitro* metabolism of urolithins in cell cultures

The stability of EA and urolithins and appearance of newly-formed metabolites in cell media was evaluated at the beginning and end of each experiment. In order to establish the role of cell metabolism on the production of ellagitannin-derived metabolites, culture media without cells were used as controls to assess chemical degradation. Different metabolic reactions, including (de)hydroxylation, conjugation with methyl, glucuronide, sulfate, cysteine, and glutathione moieties, and formation of quinones, were monitored. All the tested compounds underwent extensive biotransformations in HUVECs and THP-1-derived macrophages (Fig. 5) and fourteen newly formed metabolites were identified (Table 4). The newly-formed metabolites were detected in both cell types and the metabolic reactions were limited to sulfation and methylation (Table 4). These metabolites were not quantified due to the lack of

commercially available standard compounds, but peak area values were taken into account to establish comparisons among experiments.

In HUVECs, the stability and metabolism of EA and urolithins were studied at two different incubation times, corresponding with the study of monocyte adhesion to endothelial cells (6 h) and the secretion of sVCAM-1 and IL-6 (18 h). The molecules were stable under the experimental conditions (cell free incubations), apart from Uro D, which shown a reduced recovery even immediately after addition to the culture media. When incubated with cells, MS peak areas of the metabolites increased proportionately with incubation time. For instance, dimethyl-*O*-Uro C increased from lower limit of detection at 6 h to prominent areas after 18 h of incubation. When more than one hydroxy group was available on the molecular scaffold, isomers were often detected reflecting the number of hydroxyls present. The abundance of sulfated isomers of both Uro A and Uro C were constant, while one isomer of methyl-*O*-Uro C was produced in much higher quantities than the other. The dimethyl derivative of Uro D was predominant with respect to the monomethylated form at both 6 and 18 h, whereas the opposite occurred for EA, as the monomethylated form was higher than the dimethyl at 6 h, but not at 18 h.

In the case of THP-1-derived macrophages, a single time point was studied (24 h), but the effect of two different promoters of cholesterol accumulation (HCS and acLDL) was assessed. Again, Uro D was the most unstable molecule in cell free incubations. The production of all metabolites was elevated (between 1- and 16-fold) in the cultures containing acLDL, with respect to the HCS media (based on peak areas).

4. Discussion

The cardioprotective effect of ellagitannin-enriched diets has been related to the modulation of endothelial function as well as to hypocholesterolaemic effects [11, 12]. However, some of the *in vitro*

studies feeding ellagitannin-rich extracts have revealed that ellagitannins do not make it into the systemic circulation and therefore never reach vascular cells [7-9]. In this study, the effect of physiologically relevant ellagitannin metabolites Uro A, Uro B, Uro C, and Uro D, as well as their precursor EA, were investigated at low µM concentrations (5–10 µM) on two key events in the formation of the atherosclerotic plaques: i) endothelium activation and resulting monocyte recruitment and ii) cholesterol transport and foam cells formation. Among the tested metabolites, Uro C was the most effective, with a bioactivity similar to that of EA, while Uro A and Uro B where active in combination at 10 µM (20 µM cumulative concentration).

Endothelium activation that promotes the recruitment of circulating monocytes is one of the earliest events in the formation of atherosclerotic plaques [1]. The pro-inflammatory cytokine TNF-α, mostly produced by lymphocytes and activated monocytes/macrophages, has been implicated in the pathogenesis of a number of cardiovascular diseases, including atherosclerosis. Its production is directly linked to the activation of the endothelium, where it induces the expression of adhesion molecules, including VCAM-1, that are essential for monocyte recruitment [26]. Therefore, inhibition of its activity and, as a consequence, of endothelium activation may have an important role in the inhibition of plaque formation. Our study demonstrated that exposure of HUVECs to ellagitannin metabolites could modestly reduce the TNF-α-stimulated adhesion of monocyte to HUVECs (Fig. 1). However, this reduction reached significance only for EA and for the co-treatment of Uro A and Uro B at 10 µM.

Some effects of ellagitannin metabolites Uro A, Uro B, and their glucuronide forms on endothelial function were previously described by Giménez-Bastida et al. [17], who demonstrated that only Uro A-glucuronide has a slight effect on monocyte adhesion to endothelial cells. Their results appeared to be in accordance with the results reported herein, since neither Uro A nor Uro B as aglycone forms could significantly affect monocyte adhesion to endothelial cells at higher concentrations (18.5 µM and

14.9 μM, respectively) [17] than the ones used in the present study. As Uro A and Uro B are the two EA-derived metabolites absorbed at higher concentrations and can co-occur in some urolithin phenotypes [15, 27, 28], they were tested together. Their association was able to significantly inhibit monocyte adhesion to HUVEC (Fig. 1). Therefore, it could be hypothesized that Uro A and Uro B may exert a synergic effect on the inhibition of adhesion, as they were not active in the reduction of monocyte adhesiveness as single molecules in the present experiments, or even at higher reported concentrations [17]. However, whether the increased effect is depended on the total cumulative concentration (20 μM) of two similar molecules (10 μM Uro A+10 μM Uro B) is something that cannot be ruled out.

The proinflammatory response characterized by TNF-α-stimulated secretion of sVCAM-1 and IL-6 (Fig. 2) was counteracted by EA and Uro C at low μM concentrations (10 μM). This effect is crucial to demonstrate the atheroprotective activities of ellagitannin metabolites, since it is well established that, within the different adhesion molecules, VCAM-1 plays a major role in the early stages of atherosclerosis [29] and that sVCAM-1 secretion directly correlates with the expression of its non-soluble form on the cell surface [30, 31]. The atheroprotective effects of EA have also been confirmed in previous studies demonstrating that EA reduces endothelial activation by inhibiting monocyte adhesion to endothelial cells and the expression of ICAM-1, VCAM-1, E-selectin, and IL-6 [10, 32, 33]. The inhibition of ROS production and modulation of NF-kB activity have also be related to the anti-inflammatory effects of EA [33]. Similarly, Piwowarski et al. [16] showed that the anti-inflammatory activity of urolithins A, B, and C in RAW 264.7 murine macrophages was associated with the inhibition of NF-kB translocation into the nucleus.

Interestingly, the same molecules exerting atheroprotective effects on endothelium displayed an activity in another critical step for atherosclerotic plaque formation; specifically macrophage cholesterol accumulation. EA, Uro C, and the mixture of Uro A and Uro B reduced net cholesterol

content in human macrophages exposed to cholesterol sources, such as acLDL or HCS (Fig. 3). It was observed that these treatments caused an impairment of cholesterol uptake, without affecting cholesterol efflux (Fig. 4), despite previous data having demonstrated an effect of EA in ABCA1 expression and ABCA1 dependent-cholesterol efflux [34]. The same study reported that EA is able to block the uptake of cholesterol by macrophages exposed to oxLDL [34], which enters macrophages through scavenger receptors [1]. Nevertheless, in the present model, EA at 10 µM (Fig. 3B) did not inhibit cholesterol accumulation induced by exposition to acLDL, which represents a well-accepted experimental model of oxLDL which exploits the same scavenger receptors. In these conditions, only the association of Uro A and Uro B at 10 µM significantly reduced cholesterol accumulation. Conversely, the capacity of EA (5-10 µM) to block macrophage uptake of cholesterol derived from HCS, that is rich in non-modified LDL (native LDL) was also apparent (Fig. 3A). For the first time, it has been demonstrated that not only EA but also its metabolite Uro C is able to significantly reduce cholesterol accumulation in macrophages exposed to HCS at low µM concentration (5-10 µM). Uptake of native LDL by macrophages occurs through the LDL receptor (LDLr) or through macropinocytosis, which has been shown to induce foam cell formation and has been proposed as a new target to reduce cholesterol accumulation in atherosclerotic plaque [2, 35]. The possibility that they act by a reduction of LDLr expression or activity is unlikely because LDLr undergoes down-regulation in response to macrophage cholesterol loading [36]. Thus, it can be speculated that the mechanism underlying EA and Uro C activity is an impairment in micropinocytosis. Moreover, since these ellagitannin-derived molecules did not affect cholesterol accumulation and efflux induced by acLDL, it can be ruled out that the activity is through the scavenger receptors.

As every mammalian cell synthesizes cholesterol [25], changes in cholesterol content can also be dependent on cell specific modulation of cholesterol synthesis. An impact of urolithins on cholesterol synthesis can be excluded, as exposure to urolithins without the presence of a source of cholesterol did

not affect cell cholesterol content. However, EA caused a slightly but not statistically significant reduction in cholesterol content before addition of serum and, thus, we cannot totally exclude a possible effect of EA in cholesterol synthesis since an inhibitory activity on squalene epoxidase, a rate-limiting enzyme of cholesterol biosynthesis, has been previous described [37].

A point worth mentioning is the role the hydroxylation pattern of urolithins may have on their physiological activity [17, 38-40]. It was not possible to associate the extent of urolithin and EA hydroxylation with the anti-atherosclerotic effects observed in the present study, and this may be partly due to the extensive biotransformations undergone by the tested molecules in our cell models (Table 4, Fig. 5). It has been demonstrated that different phase II conjugates of the same urolithin may exert different biological effects [39, 41]. On the other hand, it should be noted that the metabolism of urolithins and EA by human endothelial cells and macrophages was limited to methylation and sulfation, while glucuronidation, which had previously been pointed out as one of the main reaction occurring *in vitro* and *in vivo* [20, 28], was not observed. Finally, the marked instability of Uro D in different cell cultures is something that should be better clarified in the near future, even if its bioactivity may not be affected [42].

5. Conclusions

Taken together, these results indicate that some urolithins, singularly or as mixtures, may impact key process in the development and progression of atherosclerosis. Some cellular mechanisms behind the cardioprotective features of these ellagitannin-derived metabolites have been hypothesized, but further work is needed targeting the molecular pathways involved. At the same time, *in vivo* studies aimed at unravelling the contribution of ellagitannin-containing foods to cardiovascular prevention and, in particular, to the atherosclerotic scenario, should consider clinical endpoints related to not only the anti-inflammatory response but also the lipid transport and metabolism.

From a methodological point of view, the drastic biotransformations of phenolic metabolites taking place in cell cultures should be carefully taken into account to fully elucidate the real compounds exerting the bioactivity observed. This would also help in understanding the impact of peripheral metabolism of plant-derived bioactives on human health.

Acknowledgements

This study was supported by a research grant from the US National Processed Raspberry Council. PM was funded by a grant of the Postdoctoral Fellowship Program from Fundación Séneca (Murcia Region, Spain).

References

1. Moore, K.J. and I. Tabas, *Macrophages in the pathogenesis of atherosclerosis.* Cell, 2011. **145**(3): p. 341-55.
2. Kruth, H.S., *Fluid-phase pinocytosis of LDL by macrophages: a novel target to reduce macrophage cholesterol accumulation in atherosclerotic lesions.* Curr Pharm Des, 2013. **19**(33): p. 5865-72.
3. Lusis, A.J., *Atherosclerosis.* Nature, 2000. **407**(6801): p. 233-41.
4. Crozier, A., I.B. Jaganath, and M.N. Clifford, *Dietary phenolics: chemistry, bioavailability and effects on health.* Nat Prod Rep, 2009. **26**(8): p. 1001-43.
5. Mena, P., et al., *Chapter 6 - Bioactivation of High-Molecular-Weight Polyphenols by the Gut Microbiome*, in *Diet-Microbe Interactions in the Gut*, K.T.D.D. Rio, Editor. 2015, Academic Press: San Diego. p. 73-101.
6. Anderson, K.J., et al., *Walnut polyphenolics inhibit in vitro human plasma and LDL oxidation.* J Nutr, 2001. **131**(11): p. 2837-42.

7. Aviram, M., et al., *Pomegranate phenolics from the peels, arils, and flowers are antiatherogenic: studies in vivo in atherosclerotic apolipoprotein e-deficient (E 0) mice and in vitro in cultured macrophages and lipoproteins.* J Agric Food Chem, 2008. **56**(3): p. 1148-57.
8. de Nigris, F., et al., *Beneficial effects of pomegranate juice on oxidation-sensitive genes and endothelial nitric oxide synthase activity at sites of perturbed shear stress.* Proc Natl Acad Sci U S A, 2005. **102**(13): p. 4896-901.
9. de Nigris, F., et al., *Effects of a pomegranate fruit extract rich in punicalagin on oxidation-sensitive genes and eNOS activity at sites of perturbed shear stress and atherogenesis.* Cardiovasc Res, 2007. **73**(2): p. 414-23.
10. Papoutsi, Z., et al., *Walnut extract (Juglans regia L.) and its component ellagic acid exhibit anti-inflammatory activity in human aorta endothelial cells and osteoblastic activity in the cell line KS483.* Br J Nutr, 2008. **99**(4): p. 715-22.
11. Larrosa, M., et al., *Ellagitannins, ellagic acid and vascular health.* Molecular Aspects of Medicine, 2010. **31**(6): p. 513-539.
12. Zanotti, I., et al., *Atheroprotective effects of (poly)phenols: a focus on cell cholesterol metabolism.* Food & Function, 2015. **6**(1): p. 13-31.
13. Gonzalez-Barrio, R., C.A. Edwards, and A. Crozier, *Colonic catabolism of ellagitannins, ellagic acid, and raspberry anthocyanins: in vivo and in vitro studies.* Drug Metab Dispos, 2011. **39**(9): p. 1680-8.
14. Espín, J.C., et al., *Iberian pig as a model to clarify obscure points in the bioavailability and metabolism of ellagitannins in humans.* Journal of Agricultural and Food Chemistry, 2007. **55**(25): p. 10476-10485.

15. Gonzalez-Sarrias, A., et al., *Occurrence of urolithins, gut microbiota ellagic acid metabolites and proliferation markers expression response in the human prostate gland upon consumption of walnuts and pomegranate juice.* Mol Nutr Food Res, 2010. **54**(3): p. 311-22.
16. Piwowarski, J.P., et al., *Urolithins, gut microbiota-derived metabolites of ellagitannins, inhibit LPS-induced inflammation in RAW 264.7 murine macrophages.* Molecular Nutrition & Food Research, 2015: p. n/a-n/a.
17. Giménez-Bastida, J.A., et al., *Ellagitannin metabolites, urolithin A glucuronide and its aglycone urolithin A, ameliorate TNF-α-induced inflammation and associated molecular markers in human aortic endothelial cells.* Molecular Nutrition and Food Research, 2012. **56**(5): p. 784-796.
18. Khera, A.V., et al., *Cholesterol efflux capacity, high-density lipoprotein function, and atherosclerosis.* New England Journal of Medicine, 2011. **364**(2): p. 127-135.
19. Rohatgi, A., et al., *HDL cholesterol efflux capacity and incident cardiovascular events.* New England Journal of Medicine, 2014. **371**(25): p. 2383-93.
20. Sala, R., et al., *Urolithins at physiological concentrations affect the levels of pro-inflammatory cytokines and growth factor in cultured cardiac cells in hyperglucidic conditions.* Journal of Functional Foods, 2015. **15**(0): p. 97-105.
21. Basu, S.K., et al., *Degradation of cationized low density lipoprotein and regulation of cholesterol metabolism in homozygous familial hypercholesterolemia fibroblasts.* Proc Natl Acad Sci U S A, 1976. **73**(9): p. 3178-82.
22. Brown, R.E., K.L. Jarvis, and K.J. Hyland, *Protein Measurement Using Bicinchoninic Acid - Elimination of Interfering Substances.* Analytical Biochemistry, 1989. **180**(1): p. 136-139.

23. Zanotti, I., E. Favari, and F. Bernini, *Cellular cholesterol efflux pathways: impact on intracellular lipid trafficking and methodological considerations.* Curr Pharm Biotechnol, 2012. **13**(2): p. 292-302.
24. Rader, D.J., et al., *The role of reverse cholesterol transport in animals and humans and relationship to atherosclerosis.* J Lipid Res, 2009. **50 Suppl**: p. S189-94.
25. van der Wulp, M.Y., H.J. Verkade, and A.K. Groen, *Regulation of cholesterol homeostasis.* Mol Cell Endocrinol, 2013. **368**(1-2): p. 1-16.
26. Bradley, J.R., *TNF-mediated inflammatory disease.* J Pathol, 2008. **214**(2): p. 149-60.
27. Tomás-Barberán, F.A., et al., *Ellagic acid metabolism by human gut microbiota: Consistent observation of three urolithin phenotypes in intervention trials, independent of food source, age, and health status.* Journal of Agricultural and Food Chemistry, 2014. **62**(28): p. 6535-6538.
28. Nuñez-Sanchez, M.A., et al., *Targeted metabolic profiling of pomegranate polyphenols and urolithins in plasma, urine and colon tissues from colorectal cancer patients.* Mol Nutr Food Res, 2014. **58**(6): p. 1199-211.
29. Cybulsky, M.I., et al., *A major role for VCAM-1, but not ICAM-1, in early atherosclerosis.* J Clin Invest, 2001. **107**(10): p. 1255-62.
30. Videm, V. and M. Albrigtsen, *Soluble ICAM-1 and VCAM-1 as markers of endothelial activation.* Scand J Immunol, 2008. **67**(5): p. 523-31.
31. Kjaergaard, A.G., et al., *Soluble adhesion molecules correlate with surface expression in an in vitro model of endothelial activation.* Basic Clin Pharmacol Toxicol, 2013. **113**(4): p. 273-9.
32. Lee, W.J., et al., *Ellagic acid inhibits oxidized LDL-mediated LOX-1 expression, ROS generation, and inflammation in human endothelial cells.* J Vasc Surg, 2010. **52**(5): p. 1290-300.

33. Yu, Y.M., et al., *Ellagic acid inhibits IL-1beta-induced cell adhesion molecule expression in human umbilical vein endothelial cells.* Br J Nutr, 2007. **97**(4): p. 692-8.
34. Park, S.H., et al., *Dietary ellagic acid attenuates oxidized LDL uptake and stimulates cholesterol efflux in murine macrophages.* J Nutr, 2011. **141**(11): p. 1931-7.
35. Goldstein, J.L. and M.S. Brown, *The LDL pathway in human fibroblasts: a receptor-mediated mechanism for the regulation of cholesterol metabolism.* Curr Top Cell Regul, 1976. **11**: p. 147-81.
36. Goldstein, J.L. and M.S. Brown, *The LDL receptor and the regulation of cellular cholesterol metabolism.* J Cell Sci Suppl, 1985. **3**: p. 131-7.
37. Abe, I., et al., *Ellagitannins and hexahydroxydiphenoyl esters as inhibitors of vertebrate squalene epoxidase.* J Nat Prod, 2001. **64**(8): p. 1010-4.
38. Piwowarski, J.P., et al., *Role of human gut microbiota metabolism in the anti-inflammatory effect of traditionally used ellagitannin-rich plant materials.* Journal of Ethnopharmacology, 2014. **155**(1): p. 801-809.
39. Piwowarski, J.P., S. Granica, and A.K. Kiss, *Influence of gut microbiota-derived ellagitannins metabolites urolithins on pro-inflammatory activities of human neutrophils.* Planta Medica, 2014. **80**(11): p. 887-895.
40. Giorgio, C., et al., *The ellagitannin colonic metabolite urolithin D selectively inhibits EphA2 phosphorylation in prostate cancer cells.* Molecular Nutrition and Food Research, 2015.
41. Dellafiora, L., et al., *Modelling the possible bioactivity of ellagitannin-derived metabolites. in silico tools to evaluate their potential xenoestrogenic behavior.* Food and Function, 2013. **4**(10): p. 1442-1451.
42. Gonzalez-Sarrias, A., et al., *Phase-II metabolism limits the antiproliferative activity of urolithins in human colon cancer cells.* European Journal of Nutrition, 2014. **53**(3): p. 853-64.

Figure captions

Figure 1: Effect of EA and urolithins (5-10 µM) on monocyte adhesion to endothelial cells. Mean (n=9)±SD. §§§= $p < 0.001$vs Control; *= $p < 0.05$vs TNFα.

Figure 2: Effect of EA and urolithins (10 µM) on endothelial cells secretion of sVCAM-1(A) and IL-6 (B). Mean (n=3)±SD. §§§= $p < 0.001$vs Control; *= $p < 0.05$vs TNFα, **= $p < 0.01$vs TNFα.

Figure 3: Effect of EA and urolithins (1-10 µM) on macrophage cholesterol loading. Mean (n=9)±SD. (A), HCS: Hypercholesterolemic serum; HCS cell cholesterol content (µg cholesterol/mg protein) = 20.16 ± 1.54. §§§= $p < 0.001$ vs Control, *= $p < 0.05$ vs HCS, **= $p < 0.01$ vs HCS. (B), acLDL: acetylated LDL; acLDL cell cholesterol content (µg cholesterol/mg protein) = 27.87 ± 0.71. §§§= $p < 0.001$vs Control, *= $p < 0.05$ vs acLDL ***= $p < 0.001$ vs acLDL.

Figure 4: Effect of EA and urolithins (10 µM) on macrophage cholesterol efflux. HCS: Hypercholesterolemic serum; acLDL: acetylated LDL; NCS: normocholesterolemic serum. Mean (n=9)±SD. No significant differences were detected among treatments (ANOVA $p > 0.05$).

Figure 5: Metabolic biotransformations occurring in endothelial cells and macrophages

Table 1.- Effect of EA and urolithins (10µM) on macrophage cholesterol content (µg cholesterol/mg protein) (10 µM).

Treatment	average ± SD
Control	12.94 ± 0.17
EA	11.38 ± 0.87
Uro D	13.15 ± 0.97
Uro C	15.09 ± 1.64
Uro A	12.96 ± 0.78
Uro B	13.42 ± 0.84
Uro A+Uro B	14.75 ± 1.08

Mean (n=3)±SD. No significant differences were detected among treatments (ANOVA $p > 0.05$).

Table 2.- Ellagic acid and urolithin metabolites detected in endothelial cells and/or macrophages.

Compound	Derived Metabolite	Retention time (min)	$[M-H]^-$ (*m/z*)	MS^2 ion fragments (*m/z*)	MS^3 ion fragments (*m/z*)
Urolithin B	Uro B	4.61	211	167, 182	
	Uro B-sulfate	3.75	291	211	167
Urolithin A	Uro A	3.28	227	183, 159, 199	
	Uro A-sulfate isomer 1	2.22	307	227	183
	Uro A-sulfate isomer 2	2.50	307	227	183
Urolithin C	Uro C	2.35	243	215, 199, 226	
	Uro C-sulfate isomer 1	2.13	323	243	215
	Uro C-sulfate isomer 2	2.70	323	243	215
	Methyl-*O*-Uro C isomer 1	3.39	257	242, 211, 239	
	Methyl-*O*-Uro C isomer 2	3.58	257	242, 211	
	Dimethyl-*O*-Uro C	4.43	271	256, 257	187
	Methyl-*O*-Uro C-sulfate isomer 1	2.56	337	257	214
	Methyl-*O*-Uro C-sulfate isomer 2	3.03	337	257	214
Urolithin D	Uro D	1.89	259	241, 213, 231	
	Methyl-*O*-Uro D	3.19	273	258	
	Dimethyl-*O*-Uro D	3.68	287	272, 241, 219	
Ellagic acid	Ellagic acid	1.87	301	257, 229	
	Methyl-*O*-ellagic acid	2.94	315	300	
	Dimethyl-*O*-ellagic acid	3.98	329	314, 215	

Figure 1

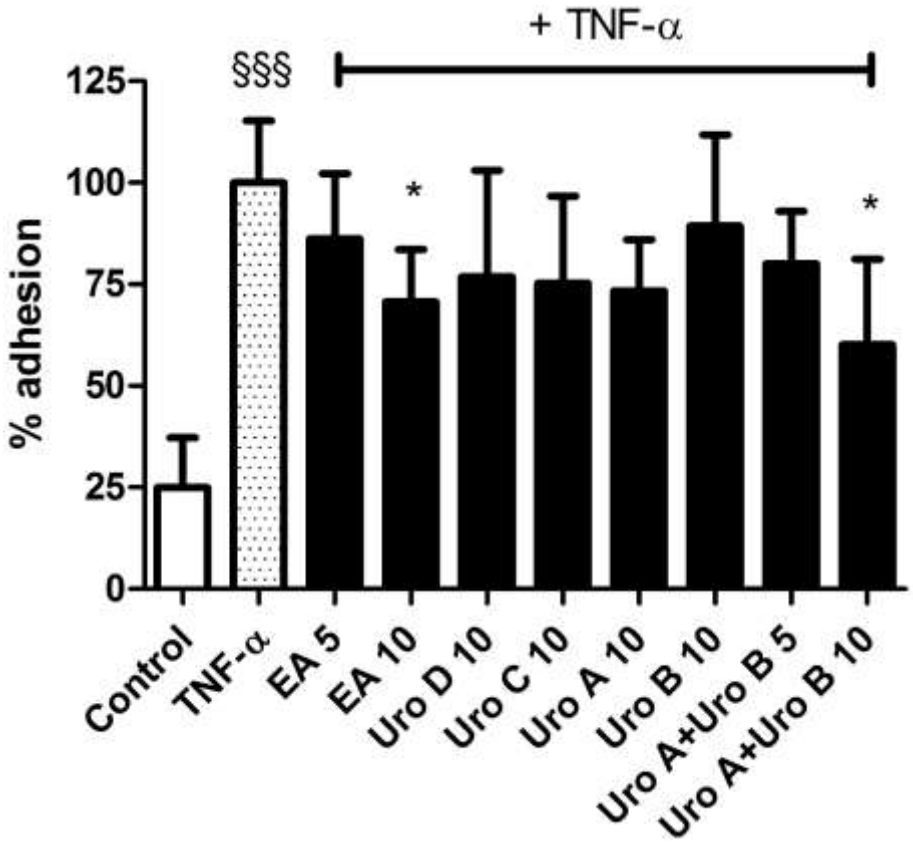
+ TNF-α
§§§
125
100
75
50
25
0
% adhesion
*
*
Control
TNF-α
EA 5
EA 10
Uro D 10
Uro C 10
Uro A 10
Uro B 10
Uro A+Uro B 5
Uro A+Uro B 10

Figure 2

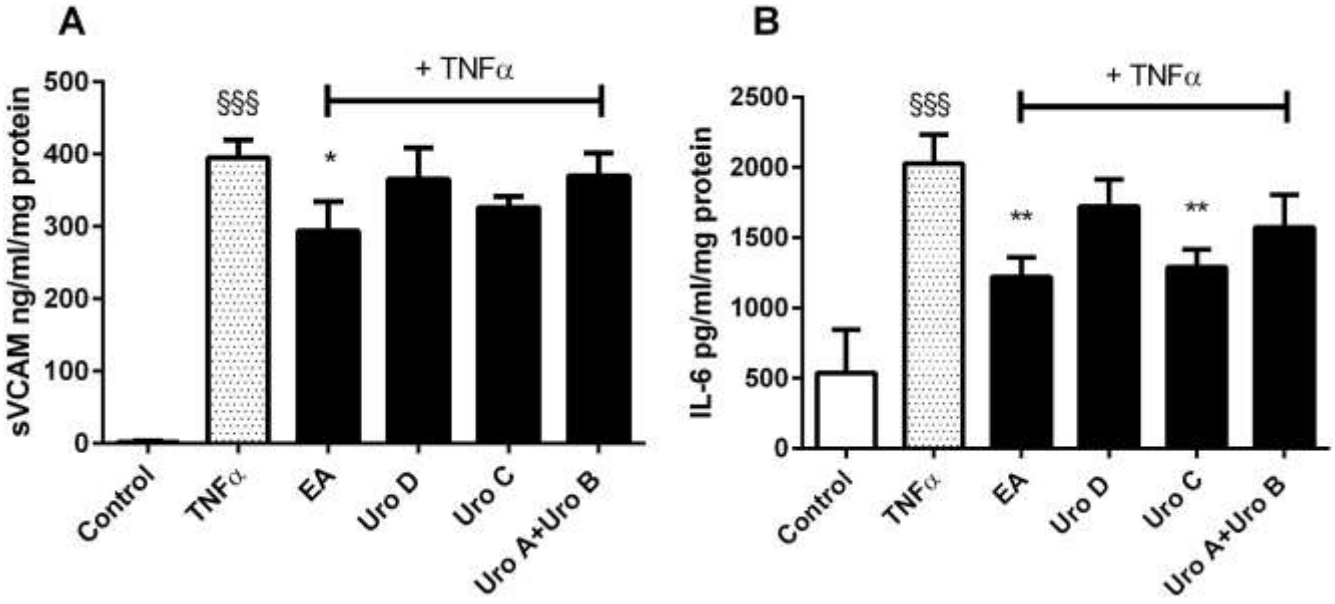
A
sVCAM ng/ml/mg protein
500
400
300
200
100
0
§§§
*
+ TNFα
Control
TNFα
EA
Uro D
Uro C
Uro A+Uro B
B
IL-6 pg/ml/mg protein
2500
2000
1500
1000
500
0
§§§
**
**
+ TNFα
Control
TNFα
EA
Uro D
Uro C
Uro A+Uro B

Figure 3

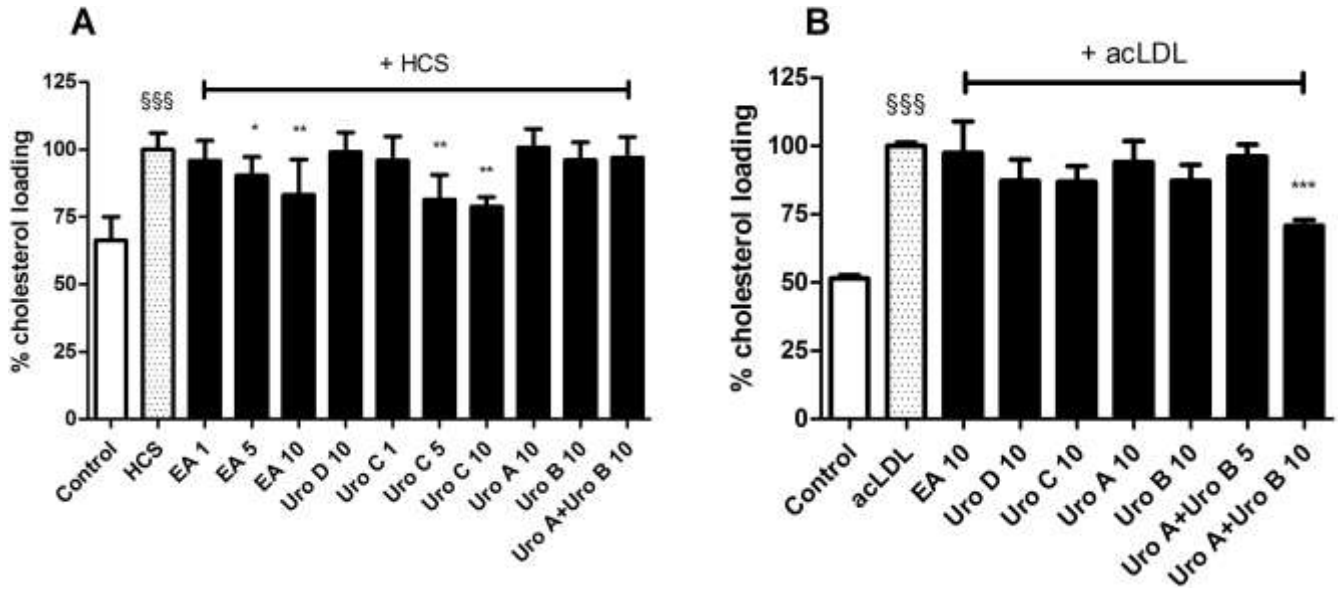
A
+ HCS
§§§
% cholesterol loading
125
100
75
50
25
0
Control
HCS
EA 1
EA 5
EA 10
Uro D 10
Uro C 1
Uro C 5
Uro C 10
Uro A 10
Uro B 10
Uro A+Uro B 10
B
+ acLDL
§§§
% cholesterol loading
Control
acLDL
EA 10
Uro D 10
Uro C 10
Uro A 10
Uro B 10
Uro A+Uro B 5
Uro A+Uro B 10

573 Figure 4

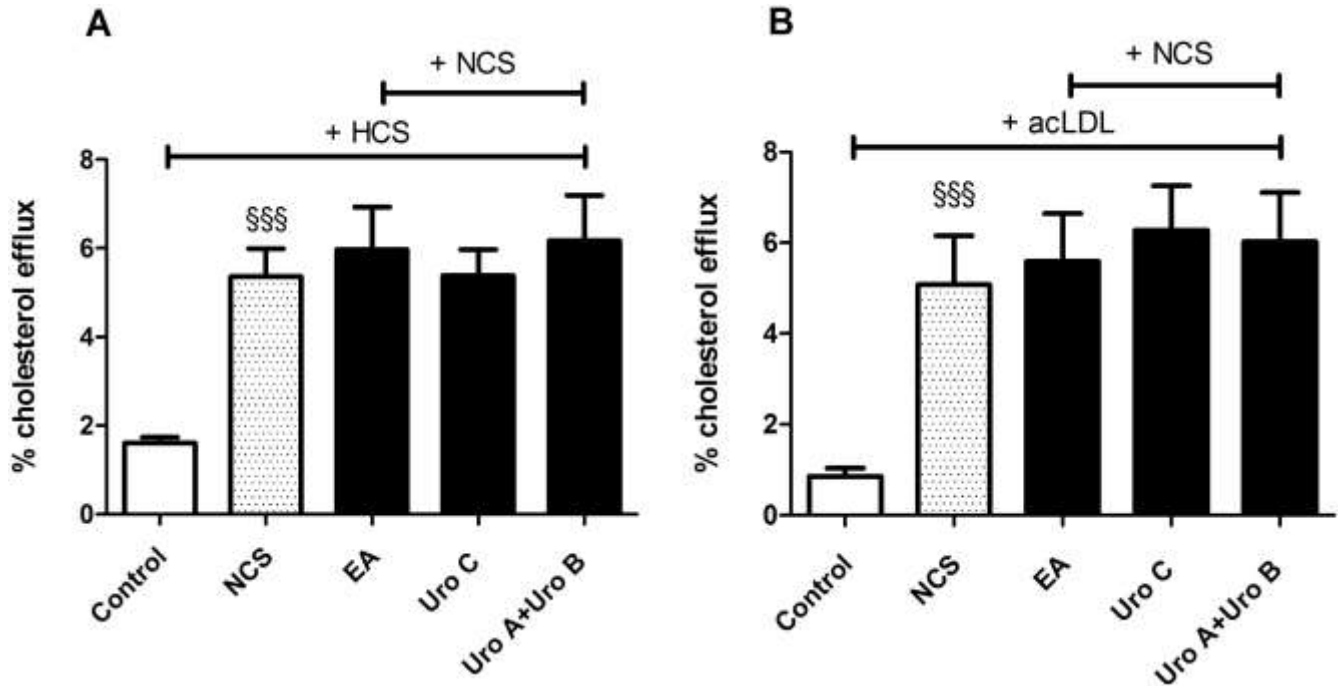

574

575

576

577

578

579

580

581

582

583

584

585

586

587

588

589 Figure 5

590

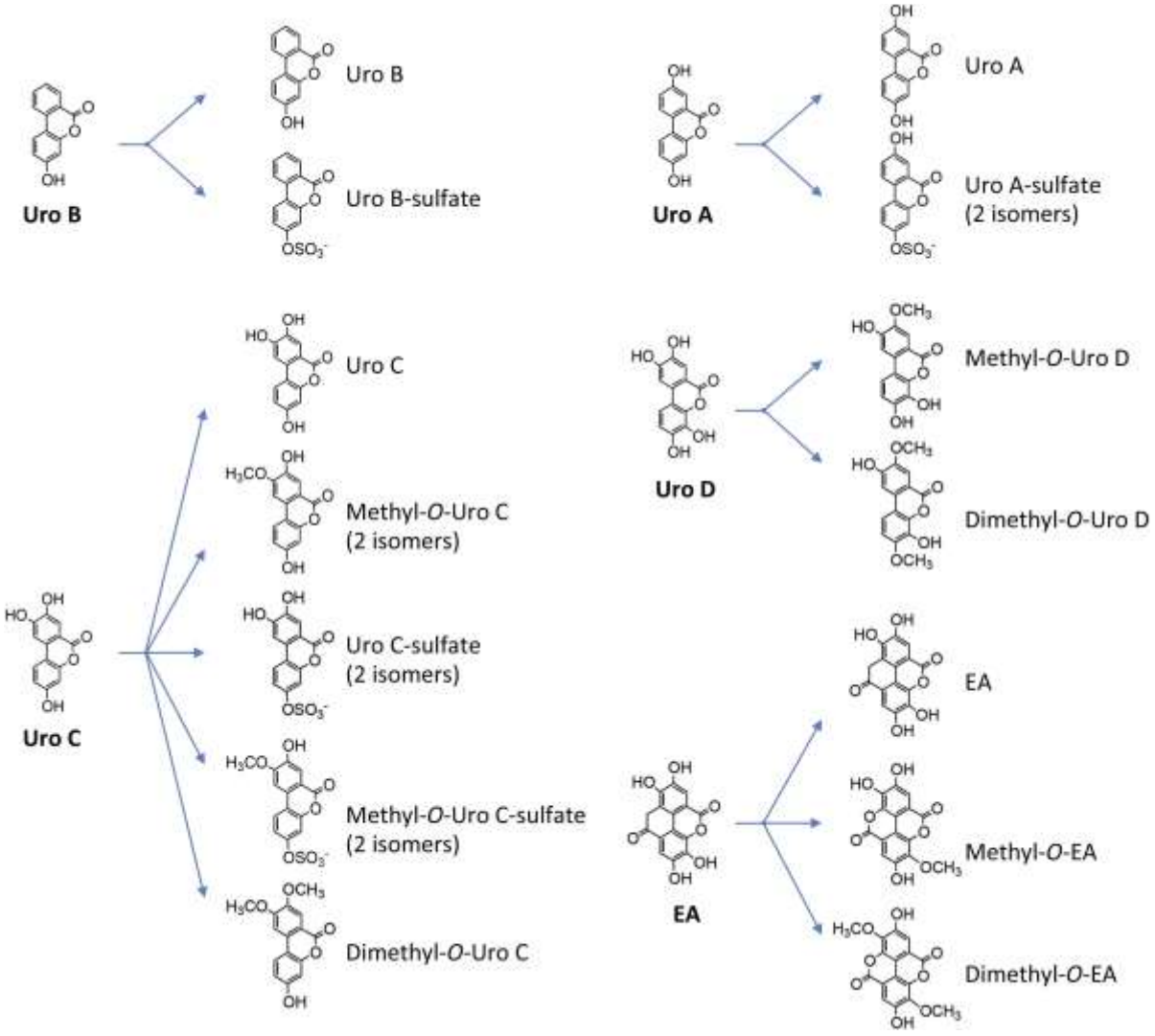

591